

A Bayesian Hierarchical Spatial Point Process Model for MS Subtype Classification

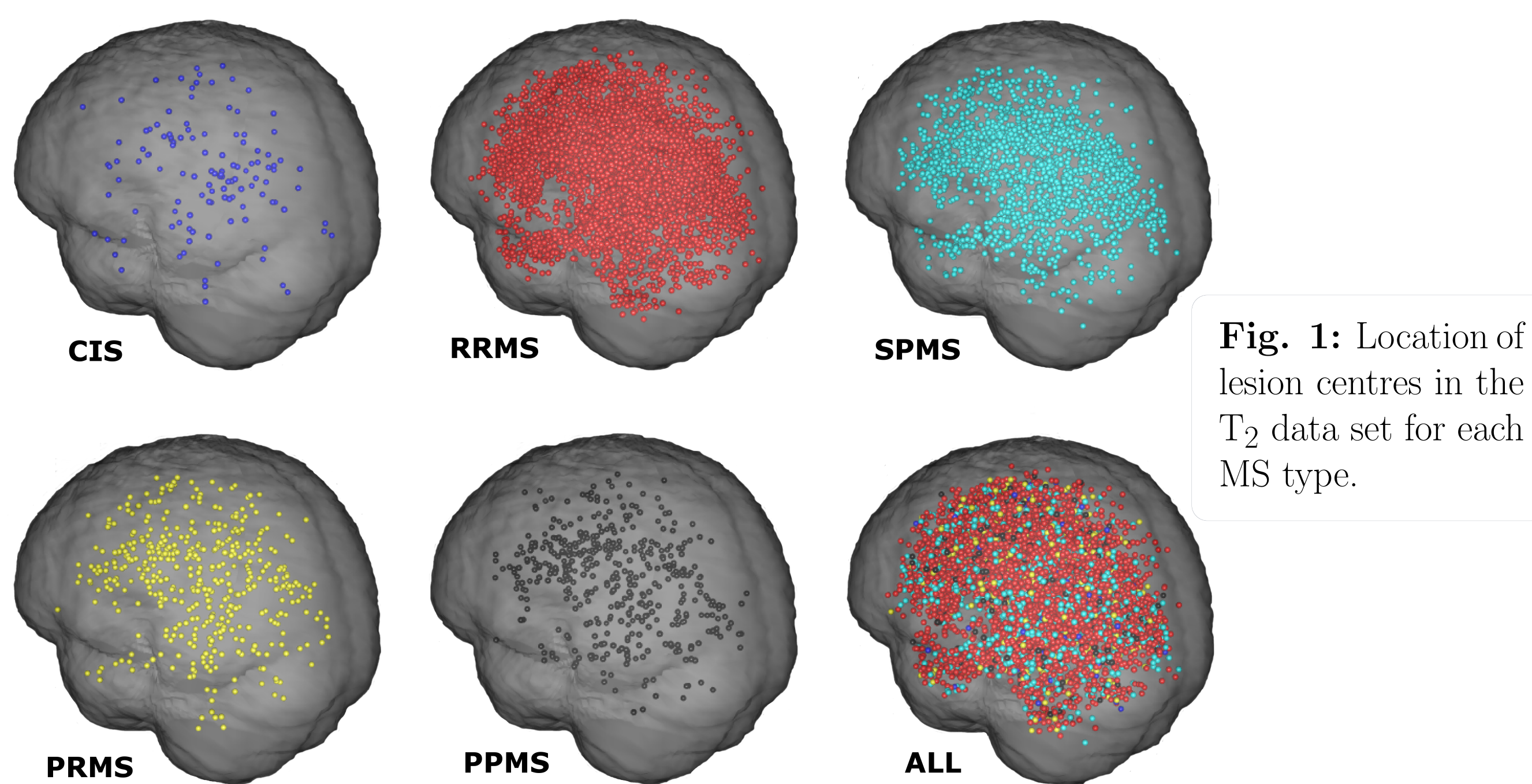
B Taschler¹, J Kang³, K Bendfeldt², E-W Radü², TD Johnson³, and TE Nichols⁴

¹Centre for Complexity Science, University of Warwick, Coventry, UK, ²Medical Image Analysis Center, University Hospital Basel, Basel, Switzerland, ³Department of Biostatistics, University of Michigan, Ann Arbor, Michigan, USA, ⁴Department of Statistics, University of Warwick, Coventry, UK.



Introduction

Multiple Sclerosis (MS) is a chronic inflammatory-demyelinating disease of the central nervous system. MS patients can be grouped into five distinct clinical categories (CIS, RRMS, SPMS, PPMS, PRMS), according to disease pathology. Currently, evaluation of MS with MRI data is largely qualitative, assessing existence and general location of lesions. We present a quantitative classification method of MS subtype using a hierarchical, fully Bayesian spatial point process model for lesion location.



Data. 259 subjects were scanned on a 1.5T Siemens Avanto scanner, collecting T₁- and T₂-weighted images; native resolution is 0.9766×0.9766×3.0mm³. Lesion masks were created in native space by a semi-automatic procedure [2] and affine registered to MNI space at 1x1x1mm³. Lesion centres of mass were then extracted using FSL; total number of lesions were 4082 (T₁) and 8866 (T₂). Clinical categorisation according to MS subgroups was CIS:11, RRMS:178, SPMS:46, PPMS:14, PRMS:10.

Hierarchical Poisson / Gamma Random Field model (HPGRF)

- A doubly stochastic Poisson point process, driven by an intensity function such that the number of points follows a Poisson distribution (Eq.1).
- Intensity is modeled as a convolution of a Gaussian spatial kernel and a Gamma random field (Eq.2) [4,1].

Model formulation. Denote a Poisson point process \mathbf{Y}_j with intensity measure $\Lambda_j(dy)$ on $\mathcal{B} \subseteq \mathbb{R}^3$ for each MS subtype j as

$$[\mathbf{Y}_j | \Lambda_j(dy)] = \mathcal{PP}\{\mathcal{B}, \Lambda_j(dy)\}, \quad (1)$$

$$\Lambda_j(dy) = \int_{\mathcal{B}} K_{\sigma_j^2}(dy, x) G_j(dx). \quad (2)$$

with $K_{\sigma_j^2}(dy, x)$ representing a type-specific (Gaussian) kernel measure.

The subtype gamma random fields $G_j(dx)$ are given by

$$[G_j(dx) | G_0(dx), \tau] \stackrel{iid}{\sim} \mathcal{GRF}\{G_0(dx), \tau\}, \quad (3)$$

$$[G_0(dx) | \alpha(dx), \beta] \sim \mathcal{GRF}\{\alpha(dx), \beta\}, \quad (4)$$

where $G_0(dx)$ represents a common, population-level gamma random field.

$$[(\mathbf{X}_j, \mathbf{Y}_j) | \{(\eta_{j,m}, \theta_m)\}, \sigma_j^2] \sim \mathcal{PP}\left\{\mathcal{B}, K_{\sigma_j^2}(dy, x) \sum_{m=1}^M \eta_{j,m} \delta_{\theta_m}(dx)\right\} \quad (5)$$

$$[\eta_{j,m} | \nu_m, \tau] \stackrel{iid}{\sim} \Gamma(\nu_m, \tau); \quad \{(\theta_m, \nu_m)\}_{m=1}^M \sim \text{invLévy}\{\alpha(dx), \beta\} \quad (6)$$

Inference. We use MCMC sampling to estimate the full posterior distribution and importance sampling [1] to estimate leave-one-out predictions.

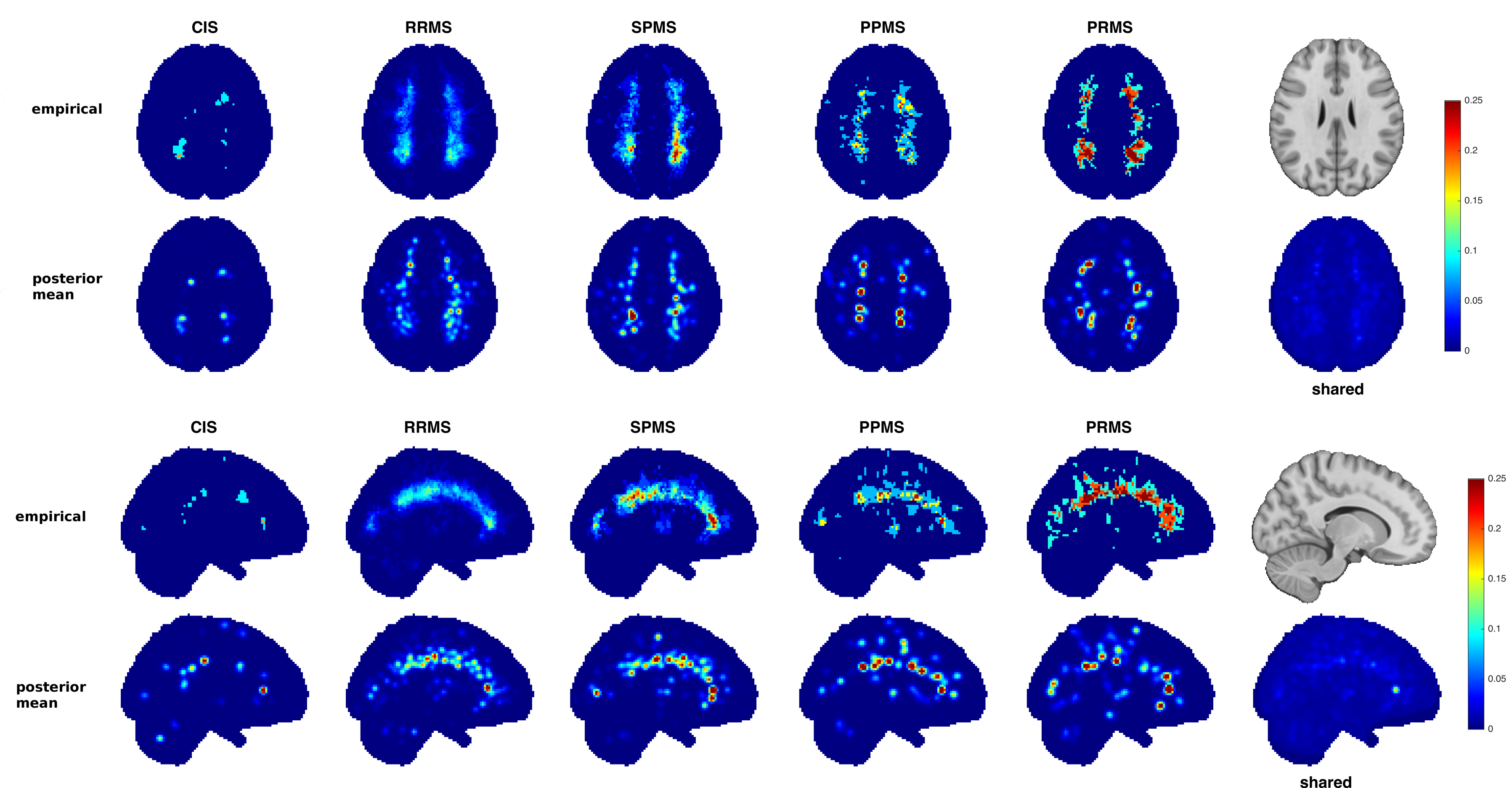
Tab. 1: T₁ data overall accuracy: 0.807; average accuracy: **0.806**.

	CIS	RRMS	PPMS	SPMS	PRMS
CIS	1.000	0.000	0.000	0.000	0.000
RRMS	0.164	0.812	0.018	0.006	0.000
PPMS	0.044	0.178	0.778	0.000	0.000
SPMS	0.000	0.154	0.000	0.846	0.000
PRMS	0.100	0.300	0.000	0.000	0.600

Tab. 2: T₂ data overall accuracy: 0.911; average accuracy: **0.906**.

	CIS	RRMS	PPMS	SPMS	PRMS
CIS	1.000	0.000	0.000	0.000	0.000
RRMS	0.073	0.927	0.000	0.000	0.000
PPMS	0.065	0.087	0.848	0.000	0.000
SPMS	0.000	0.071	0.071	0.857	0.000
PRMS	0.000	0.100	0.000	0.000	0.900

Fig. 2: Empirical probability and estimated mean posterior intensity maps (T₂ data).



Results

2D-slices of estimated mean posterior intensity maps across all subtypes are shown in Fig.2. Similar patterns occur especially for RRMS and SPMS subtypes, which are also clinically linked. The computed intensities are consistent with empirically obtained binary lesion maps. Confusion matrices (Tables 1 & 2) resulting from LOOCV show high classification accuracies of over 80% for T₁ and 91.1% for T₂ data, respectively.

Importantly, our spatially informed model performs better than a machine learning approach using support vector machine (56%) as well as a full-image probit regression model (82%); for details see [3].

Further extensions

Due to its non-parametric nature, the HPGRF model provides greater flexibility in estimating the intensity function than parametric approaches. Despite using only lesion location, it has accuracy similar to using all image data; while being less dependent on exact lesion segmentation. Current work is focused on incorporating (constant or spatially varying) covariates into the model; as well as including ‘marks’ on individual lesion locations.

References

- [1] Kang J, et al. (2014), *Ann of Appl Stat* 8 (3): 1800-1824.
- [2] Kappos L, et al. (2006), *NEJM* 335 (11): 1124-1140.
- [3] Taschler B, et al. (2014), *LNCS - MICCAI 2014* 8674: 797-804.
- [4] Wolpert RL, et al. (1998), *Biometrika* 85 (2): 251-267.

